Preparation and characterization of PES-based membranes : impact of the factors using a central composite an experimental design

NATHALIE KOBBE DAMA[1,2,3], ANTHONY SZYMCZYK[3], ANTOINE ARFAO TAMSA[1], JEAN BOSCO TCHATCHUENG[2]

[1]Process Engineering, Saint Jerome Polytechnic, Saint-Jerome Catholic University Institute of Douala, Douala, CAMEROUN

[2]Department of Applied Chemistry, ENSAI, University of Ngaoundere, Ngaoundere, CAMEROON,

[3]Univ Rennes, CNRS, ISCR (Institut des Sciences Chimiques de Rennes) – UMR 6226, F-35000 Rennes, FRANCE

kobbedamanathalie@yahoo.fr

Abstract:- In this work, PES (polyethersulfone) /PVP (Polyvinylpyrrolidone) blend membranes and PES (Polyethersulfone) /ZnO (Zinc Oxide) mixed-matrix membranes (MMMs) were fabricated by a phase-inversion method. The membranes were characterized by several techniques including FTIR-ATR, porosity, water permeability and membrane performance in lysozyme solution (0.35 g/L). It was revealed that the casting speed influences the permeability of these membranes with variation rate of 67% for casting speed 20 and 30 mm/s. The porosity increases with the addition of PVP and ZnO nanopartticles (NPs). The porosity of PES/PVP membranes and PES/ZnO MMMs increased by 246% and 31% with respect to that of the PES membrane by adding PVP and ZnO NPs, respectively. Water flux of PES/ZnO hybrid membranes (with 0.5% of added ZnO NPs) significantly improved after the addition of ZnO NPs of 170%. The lysozyme rejection performance at 3 bar was found similar for the PES and PES/PVP membranes (85% and 86%, respectively) and slightly lower (75%) for the PES/ZnO hybrid membranes. The optimal permeability of 17.7 $L.h^{-1}.m^{-2}.bar^{-1}$ was achieved with solvent and ZnO NPs percentages of 70% and 0.5%, respestively, and a casting speed of 20 mm/s.

Key-words : - polyethersulfone membrane, polyvinylpyrrolidone, ZnO nanoparticles, phase inversion, mixed-matrix membranes, optimal permeability

1 Introduction

Polyethersulfone (PES) is a kind of polymer with good performance and widely used for microfiltration (MF), ultrafiltration (UF), nanofiltration (NF) and gas separation application [1-4]. It has lots of merits like high temperature and good chemical resistance, wide pH tolerance, easy to be fabricated into membranes with a broad range of pore sizes and different configurations. Phase inversion process is the most common used method for the preparation of PES membranes. In this process, a homogeneous solution is first formed, then immersed in a non-solvent bath to form the membrane [5, 6].

However, the PES membranes performance in aqueous phase is limited as a result of their relative high hydrophobicity. Moreover, when solutions containing proteins or other hydrophobic substances are filtered, fouling phenomenon occurs and the flux permeation of membrane highly decreases [2, 7, 8]. A useful technique to overcome this limitation is to enhance the membrane hydrophilicity by blending PES with hydrophilic additives. The blending of a hydrophilic polymer as an additive in the PES membrane offers new properties to the membrane [9, 10]. Among the commonly hydrophilic additive used to improve its performance, is polyvinylpyrrolidone (PVP) which makes the membrane also more porous [4].

One of the major locks of membrane processes is fouling. In order to optimize the performance of the membranes and to inhibit the proliferation of microorganisms, cycles of cleaning and disinfection with chemicals are therefore regularly performed. Sodium hypochlorite (NaOCl) is promising disinfectant because of its performance and cost effectiveness. However, it can cause premature aging of membrane materials and in particular significant oxidation of PVP [11, 12].

Therefore, substantial efforts have been made to prepare membrane with proper morphology and characteristics to mitigate membrane fouling and

aging. In order to mitigate PES membrane fouling, several appoaches such as blending with hydrophilic polymer [7, 13] , grafting with hydrophilic monomers [14, 15], grafting with short-chain molecules [16], embedding hydrophilic nanoparticles, etc. have been suggested [8].

Blending polymers with inorganic nanoparticles has attracted incerased attention because of convenient and mild synthesis conditions required for the preparation of membrane. Beneficial effects of nanoparticles on membrane characteristics have been reported such as the amelioration of surface hydrophilicity and enhancement of antifouling property [8]. In addition, many types of nanoparticles have been studied to improve the membrane properties, such as silica (SiO_2), silver (Ag), zirconia (ZrO_2), gold (Au), zerovalent iron (Fe^0), palladium (Pd) and ZnO [17].

Zinc oxide, as one of the low cost and multifunctional inorganic nanoparticles, has drawn increasing attention due to the prominent physical and chemical properties, such as high catalytic activity, and effective antibacterial and bactericide capabilities [18, 19]. In addition, high hydrophilicity of ZnO nanoparticles has made them as one of most suitable materials for improvement of the hydrophilicity of composite membranes. As a result of high surface area, ZnO nanoparticles can easily absorb hydrophylic hydroxyl groups (-OH) to become hydrophilic [20]. Moreover, ZnO nanoparticles can be suitably embedded in a membrane to develop a stable operating system with simultaneously improved physical and chemical properties. Thus, the incorporation of ZnO nanoparticles in the membrane matrix is a promising approach that might solve the fouling problem of membrane.

Several studies have tried to improve the properties of PES membranes [21]. Recently, attention has been focused on amelioration of some key factors for the casting solution system. moreover, addition of ZnO resulted in an improvement in hydrophilicity , compaction resistance, thermal stability and antifouling property of membrane. A few studies have been done on the permeation, influence of the casting speed, reproduction of membrane, porosity and membrane filtration. The main objective of this study is to develop high performance PES-based membranes and to assess the main factors influencing the membrane performance by central composite an experimental design.

2 Experimental

2.1 Materials

Polyethersulfone (PES Veradel 3000 MP) in powder form. NMP (1-methyl-2-pyrrolidone) from Fluka analytical and PVP (polyvinylpyrrolidone, MW = 40.000g/mol) from Riedel-de Haen were used in the casting solution as solvent and pore former, respectively. ZnO nanoparticles were purchased from Riedel-de Haen. Deionized water was used for coagulation bath. The support layer (Viledon FO2471) used for the PES membrane manufacturing was obtained from Freudenberg (Weinheim, Germany). The property and chemical structure of polyethersulfone (PES), polyvinylpyrrolidone (PVP), 1-methyl-2-pyrrolydone (NMP) and lysozyme are illustrated in Table 1 and Fig. 1 respectively.

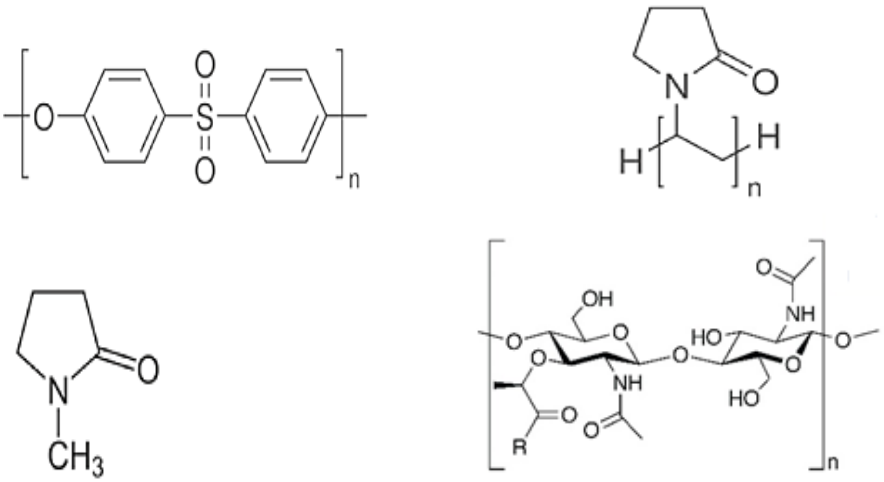

Fig. 1. Chemical structure of **(a)** polyethersulfone (PES), **(b)** polyvinylpyrrolidone (PVP), **(c)** 1-methyl-2-pyrrolydone (NMP) and **(d)** Lysozyme

Reagents	Manufactures	Molecular weight ($g.mol^{-1}$)	Purity (%)
Polyethersufone (PES) (PES VERADEL 3000 MP)	/	35 000	/
1-methyl-2-pyrrolidone (NMP) (C_5H_9NO)	Riedel-de Haen	99.13	99
Polyvinylpyrrolidone (PVP)	Fluka analytical	40 000	/
Zinc Oxyde (ZnO)	Riedel-de Haen	81.41	/
Sodium Metabisulfite ($Na_2S_2O_5$)	Acros Organics	190.1	97
Lysozyme	Acros Organics	14 300	/

Table 1. Characteristic of the products used

2.2 Membrane preparation method

All membranes were prepared using the phase-inversion method [8].

Different amounts of PVP or ZnO NPs were added into NMP (solvent) and the solutions were subsequently stirred for 1h at 250 rpm and room temperature to obtain a homogenous mixture. Then, PES (25 wt%) was added and the solutions were strirred for 24h at 250 rpm and room temperature.

The collodion were further casted on a glass plate using an automatic film applicator (Elcometer K4340) with a 200 μm casting knife. Then, the casted solution was immediately immersed into a non-solvent bath (deionized (DI) water) at room temperature for precipitation. The so-obtained membranes stored in DI water for 24h to ensure total solvent removal. Finally, the membranes were stored in a sodium metabisulphite ($Na_2S_2O_5$) solution (5g/L) until use. The composition of the various casting solutions is given in Table 2.

Membranes	PES (wt%)	NMP (wt%)	PVP (wt%)
PES	25	75	0
PES/PVP	25	72	3
PES/ZnO	25	74.5	0.5

Table 2. The compositions of casting solutions

2.3 Filtration experiments

2.3.1 Filtration setup

The membrane performance was analyzed by dead-end filtration using a cell of volume V = 300 mL.

The effective membrane surface area was 45.4 cm^2. The transmembrane pressure was applied by means of a nitrogen gas source. The permeate was collected in a beaker and weighed in order to determine the permeation flux of the membrane. The membranes were initially compacted at a transmembrane pressure of 5 bar for 1 h. Permeability measurements were conducted at room temperature and the pressure was varied from 1 to 5 bar.

2.3.2 Water flux and rejection measurement

The water flux was measured after 2 min of water filtration. Water flux (Jw) was calculated according to Eq. (1).

$$J_w = \frac{Q}{A \times \Delta t} \quad (1)$$

Where Q is the mass of water collected in the permeate compartment. A is the effective surface area of the membrane, and Δt is the time of the measurement. [20].

Fouling experiment were carried out with a lysozyme solution (0.35 g/L) in order to assess the (anti)fouling properties of PES. The permeate flux decline with filtration time was measured at 3 bar for 60 min operation. After 15 min of filtration, the lysozyme concentration in the feed solution and permeation solution were measured, respectively. The rejection was calculated according to Eq. (2).

$$R(\%) = \left(1 - \frac{C_p}{C_f}\right) \times 100 \quad (2)$$

Where C_p is the lysozyme concentration (g/L) of the permeation solution and C_f is the lysozyme concentration (g/L) of the feed solution. The lysozyme concentration was measured with UV-VIS spectroscopy at $\lambda_{max} = 280\ nm$ [22].

2.4 FTIR spectroscopy

After careful dynamical vacuum drying (two days) the top surface of membrane samples was characterized using a FT/IR-4100 Fourier Transform Infrared Spectrometer (Jasco) equipped with a ZnSe crystal ATR element (single reflection; incidence angle: 45°). Spectra were collected from 600 to 3700 cm^{-1} at 2 cm^{-1} resolution and each spectrum was averaged from 128 scans after background recording performed at ambient air.

2.5 Porosity measurements

The porosity (ε) was determined by gravimetric method, difined as:

$$\varepsilon = \frac{W_w - W_d}{\rho_w . A . l} \quad (3)$$

Where W_w is the weight of the wet membrane;W_d is the weight of the dry membrane; ρ_w is the wáter density (998 kg.m^{-3}); A is the effective area of the membrane (3 cm^2); l is the membrane thickness (m). [23].

2.6 Experimental Design: Central Composite Designs

It has been reported in the literature that numerous factors can influence permeability [9, 10, 24, 25]. To assess key parameters for better permeability efficiency, Central Composite Designs was used [26, 27]. A 3-factor, two levels plus center points central composite an experimental design matrix was used to investigate the effects of selected parameters are listed in Table 3.

Natural levels of the design factors	Coded levels of the design factors		
	(-1)	0	(+1)
X_1: NMP (%)	70	75	80
X_2: ZnO (%)	0.5	1	1.5
X_3: Casting speed (mm/s)	20	30	40

Table 3. Natural and coded levels of the design factors

The response function was the permeability. The postulated quadratic polynomial model to Eq. 4 generally enables the description of several studied responses in a reasonable experimental domain.

$$Y_{Permeability} = a_0 + \sum a_i X_i + \sum a_{ij} X_i X_j + \sum a_{ijk} X_i X_j X_k \quad (4)$$

Where $Y_{permeability}$ = permeability water, a_0 = estimation of average responses, a_i = estimation of main effects of variables I, a_i = estimation of quadratic effects of variables i, a_{ij} = estimation of interactions between variables i and j, a_{ijk} = estimation of interactions between variables i, j and k.

Calculation of the different coefficients a_i, a_{ij}, aijk, was done according to the least squares method using Eq. (5).

$$a_i = (X'X)^{-1} . X' . Y \quad (5)$$

where X = matrix of model, X' = transposed matrix of X, (X' X) = matrix of information,

(X' X)$^{-1}$ = matrix of scattering, Y = vector of experiment responses.

Microsoft Excel 2015 and Minitab plus software were used to analyse the obtained data.

Estimating the weight of different factors and their interactions on the response.

To estimate the weight of the different variables and their interactions on the response, Pareto analysis [28]. Method which expresses the effect of Xi parameter by relation was used.

$$F_i = 100\left(a_i^2 / \sum a_j^2\right) \quad (6)$$

Where F_i = percentage of the effect of parameter i on the response, a_i^2 = quadratic estimation of coefficient of variable i, $\sum a_j^2$= sum of quadratic estimations of all coefficients

3 Results and discussion

3.1 Influence of casting speed

Influence of the casting speed (20-50mm/s) on membrane properties was studied.

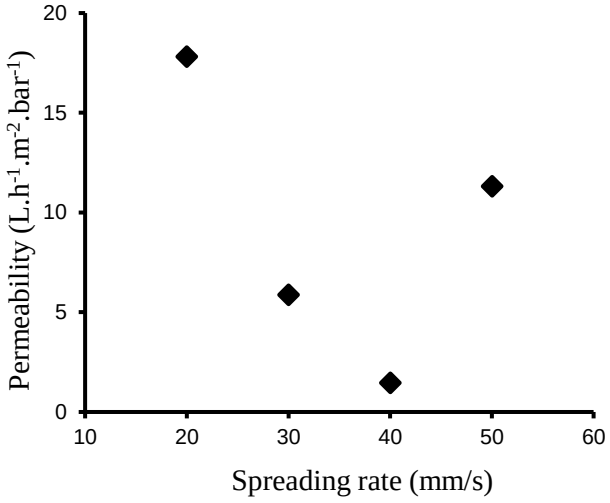

Fig. 2. Pure water permeability of (pure) PES membrane as a function of the casting speed

Fig. 2 shows a point cloud of membrane permeability in pure PES versus velocity. The

permeability tests were carried out at a constant pressure of 3 bar. The lower permeability, 1,5 $L.h^{-1}.m^{-2}.bar^{-1}$, was obtained for a casting speed of 40 mm/s whereas the highest permeability, 17.8 $L.h^{-1}.m^{-2}.bar^{-1}$ was obtained at 20 mm/s.

It was revealed that the casting speed influences the permeability of membranes. For speeds lower than 20 mm/s, the exchanges between the ambient air and the collodion are important. To avoid the evaporation of the solvent and the absorption of water from ambient air, the polymer films were immediately immersed into the non-solvent bath. The casting speed also affects the membrane morphology, porosity and pore size by which is attributed to the alternation of molecular orientation caused by induced shear rate [24].

3.2 Membrane characterization

In order to study the chemical structure and composition of the membrane. FT-IR spectrum of different compositions of PES-PVP membrane were also evaluated and results presented in Fig. 3. As already reported in literature, FT-IR spectrum of PES demonstrated absorption bands at 3470, 2800-2900, 1750, 1380, 1233, 1047 and 886 cm^{-1} which correspond to O-H, C-H, C=O and C-O stretching vibration [29].

The band at 1674 cm^{-1} is assigned with the PVP [25, 29].

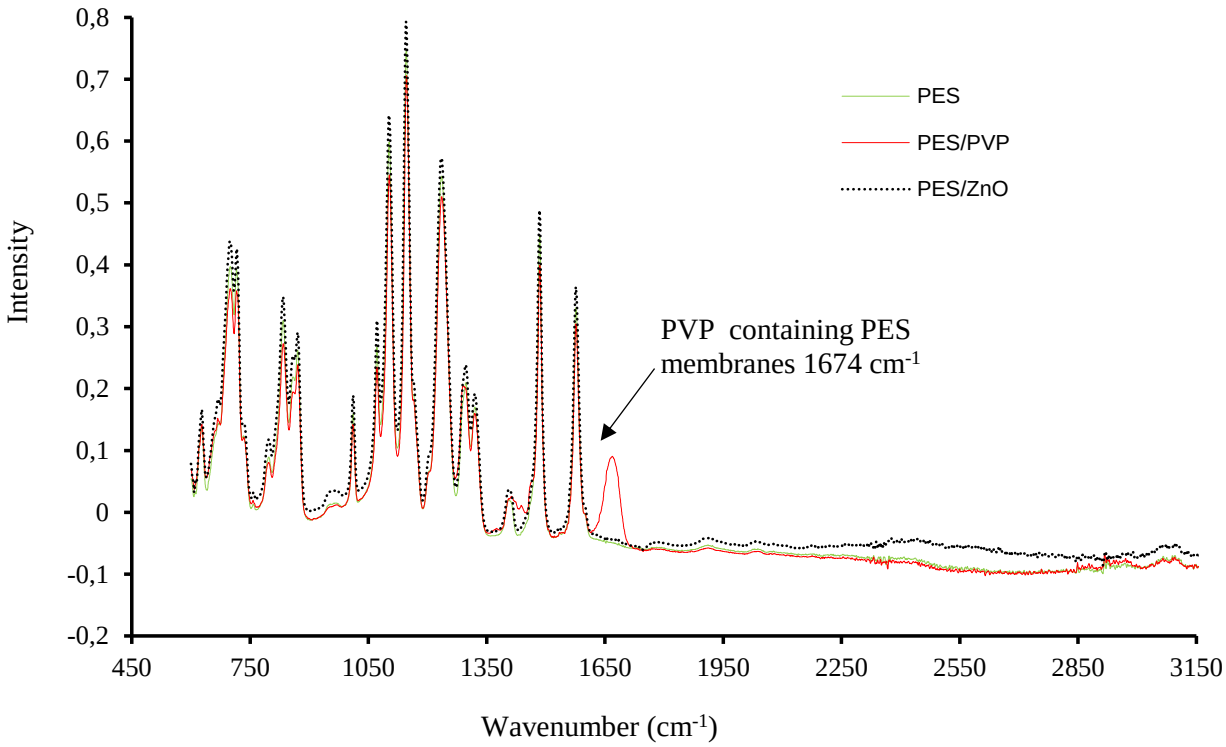

Fig. 3. FTIR spectra of PES ; PES/ZnO and PES/PVP membranes

On the spectrum, we can also observe the presence of an absorption band at 1050 cm^{-1} which corresponds to the C - 0 - C backbone of the PES. This last band proves that the PES is not degraded during the formation of PES/ZnO.

The porosity of each membrane was obtained by volume fraction of the membrane.

In Fig.4, the porosities of PES/PVP and ZnO/PES hybrid membranes are higher than that of the PES membrane. The porosity increases with increasing weight of added PVP and nano-ZnO. It is known that high porosity is favorable to water flux. It is generally accepted as a common rule that the enhanced exchange rate between water and solvent can make more porous membranes and vice versa [21, 23]. The reasons for the porosity variable can be explained below. The presence of nano-ZnO generates two effects: hydrophilicity effect and viscosity effect. Hydrophilic nano-ZnO easily draws water into the casting suspension in the phase

inversion process. The hydrophilicity effect can increase the exchange rate between water and solvent. When the weight of added PVP and nano-ZnO, the viscosity of the casting suspension is high that the hydrophilicity effet is dominant [8, 22, 30].

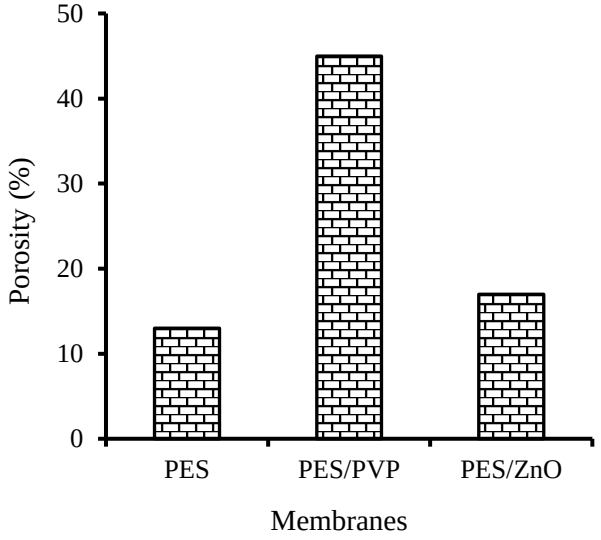

Fig. 4. Porosity of the various membrane

Shen et al [20] believed, the higher the nano-ZnO addition weight leads to higher viscosity. When the weight of nano-ZnO added is high (more than 0.5%), the viscosity of the casting slurry is so high that the viscosity effect dominates the hydrophilic effect. The reduced exchange rate results in decreased porosity. The porosity variable is affected by these two effects.

3.3 Flux and rejection

The cross-flow system was used to measure the filtration properties of membranes at 25 °C. After studying the influence of the spreading speed, we was decided to work with a casting speed in the middle of this range, whether 30 mm/s. Filtration properties of all the prepared membranes are shown in Fig. 5. The water permeabilities of the PES/PVP and PES/ZnO hybrid membranes are higher than of the PES membrane and reach 8.1 and 15.2 $L.h^{-1}.m^{-2}.bar^{-1}$, respectively. The low addition weight of nano-ZnO leads to a small viscosity. The increased exchange rate results in raise permeability [20]. This flux represents an improvement of 170% over that of the PES membrane.

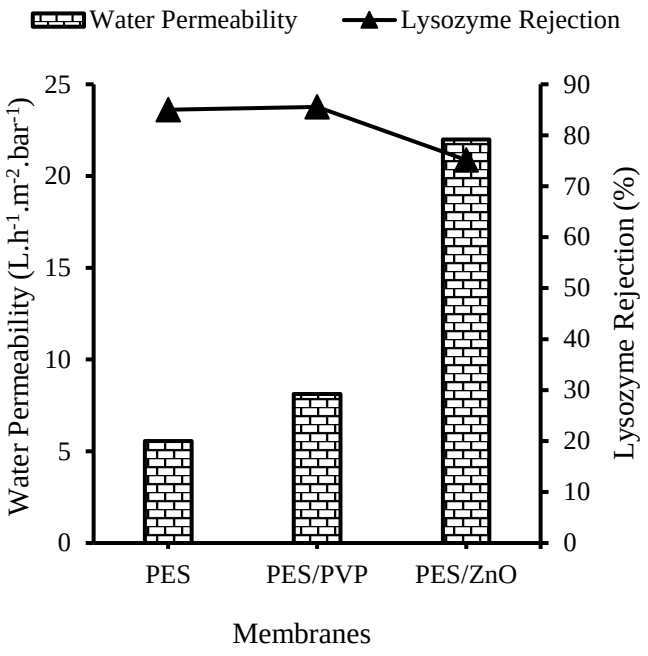

Fig. 5. Water permeability and lysozyme rejection of PES, PES/PVP and PES/ZnO

In order to estimate the rejection performance of the PES, PES/PVP and PES/ZnO membranes, lysozyme (0.3 g/L) were used. Fig. 5 shows a typical tendency for the rejection of lysozyme by membrane. The results of the rejection performance showed that our membranes have a retention rate of lysozyme of 85% for PES, 75% for PES/ZnO and 86% for PES/PVP. These result suggest that the addition of ZnO NPs did not lead to substantial modification of the membrane pore size.

3.4 Dominants Factors

Table 4 presents the three factor of central composite design with corresponding experimental responses and predicted values of permeability. Equation (4) has been used to observe the effects of experimental factors on permeability. Experimental values are measured for a particular run, and the predicted values are evaluated from the quadratic polynomial model and are generated by using the approximating functions. These results are analyzed by the linear regression method as recommended by the method used. Estimations of quadratic model coefficients are presented in table 5. Pareto analysis is presented in Fig. 6.

Run	Factors (coded values)			Permeability ($L.h^{-1}.m^{-2}.bar^{-1}$)		
	X_1	X_2	X_3	Experimental	Predicated	Residue
1	70	0.5	20	17.72	18.3	0.58
2	80	0.5	20	3.24	2.6	-0.64
3	70	1.5	20	11.85	10.5	-1.35
4	80	1.5	20	14.12	13.8	-0.32
5	70	0.5	40	17.23	18.2	0.97
6	80	0.5	40	4.32	5.1	0.78
7	70	1.5	40	11.58	10.3	-1.28
8	80	1.5	40	4.97	5.2	0.23
9	75	1	30	2.78	2.6	-0.18
10	75	1	30	2.53	2.6	0.07
11	75	1	30	2.67	2.6	-0.07
12	75	1	30	2.49	2.6	0.11

Table 4. Design matrix and results of the central composite design

regression method as recommended by the method used. Estimations of quadratic model coefficients are presented in table 5. Pareto analysis is presented in Fig. 6.

Factors and interactions	Coefficients a_i	Pareto analysis $\%a_i$
X_1	-3.96	34.48
X_2	0.01	0.10
X_3	-1.11	9.71
$X_1 X_2$	2.89	25.20
$X_1 X_3$	-0.92	8.05
$X_2 X_3$	-1.26	10.99
$X_1 X_2 X_3$	-1.32	11.47
a_0=10.64		

Table 5. Coefficients a_i of the models and Pareto analysis

The coefficients for the linear, quadratic and interactive terms were evaluated using Minitab17 as follows: - 3.96, 0.01, - 1.10, + 2.88, - 0.91, - 1.25 and -1.31 for X_1, X_2, X_3, X_1X_2, X_1X_3, X_2X_3 and $X_1X_2X_3$ respectively.

The plot of pareto analysis [32] (Fig. 6) indicates that the coefficients for linear effect of ZnO NPs (X_2), casting speed (X_3), interaction between ZnO NPs and casting speed (X_1X_3) were found to be insignificant (percentage of influence < 10%) indicating that these parameters do not affected the permeability. But the coefficients of the solvent (X_1), interaction between solvent and ZnO NPs (X_1X_2), interaction between ZnO NPs and casting speed (X_2X_3), interaction between solvent, ZnO NPs and casting speed ($X_1X_2X_3$) were found to be the most significant with percentage of influence on the response of 34.48%, 25.20%, 10.99% and 11.47% respectively.

It is the factor X_1, the solvent, which is the most influential. X_2 and X_3 are not directly influential, but they are through their interactions. The solvent has a major impact on the permeability. The porosity of the membrane increases with the concentration of solvent (finger-like structure) and decreases with the decrease of the solvent concentration (sponge-like structure): the increase in the mass concentration of polymer causes a drop in the flow of permeability of membranes [33-34]. The interaction between the solvent and ZnO NPs showed that there was an influence on the structure of the membranes. That would correspond to the increase of the viscosity of the collodions and a good dispersion of the ZnO NPs in the membrane matrix [34].

Thus attention must be paid not only on main effects but also on interaction parameters. Multiple regression analysis equation obtained is as follows:

$$\mathbf{Y_{Permeability}} = 10.64 - 3.96X_1 + 0.01X_2 - 1.11X_3 + 2.89X_1X_2 - 0.92X_1X_3 - 1.26X_2X_3 - 1.26X_1X_2X_3 \quad (7)$$

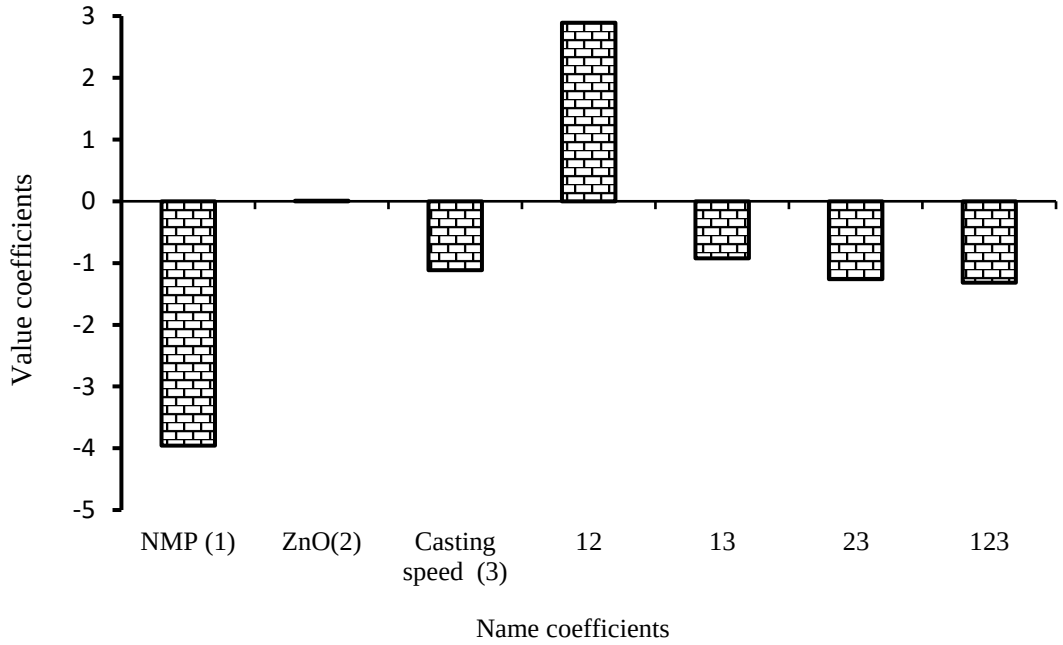

Fig. 6. Pareto analysis of the weights of the models terms

The plot of pareto analysis [32] (Fig. 6) indicates the two positive effect of the parameters X_2, X_1X_2 on the permeability and fine negative effects of the parameters X_1, X_3, X_1X_3, X_2X_3, $X_1X_2X_3$ on the permeability of the membrane. The coefficient b_2 of the model is positive, coefficients b_1 and b_3 are negative indicating respectively that increasing the value of X_2 increases the permeability and increasing the value of X_1 or X_3 decreases the permeability. Interaction coefficient b_{12} is positive and b_{13}, b_{23} are negative; the interaction of X_1X_2 increases the permeability of membrane whereas the interaction of X_1X_3 or X_2X_3 reduces the permeability of membrane.

A simple method to validate the above equation of the model is to compare the experimental responses the calculated responses (Fig. 7). The coefficient (0.99) of this regression curve indicates that there is not significant different between the experimental response and the calculated responses and thus the model is validated.

The response surfaces in Fig. 8 (a, b, c) indicate that the solvant (X_1) affects the permeability, the ZnO NPs (X_2) also affects the permeability but in a lesser degree than solvant dose whereas the casting speed (X_3) slightly affects this response.

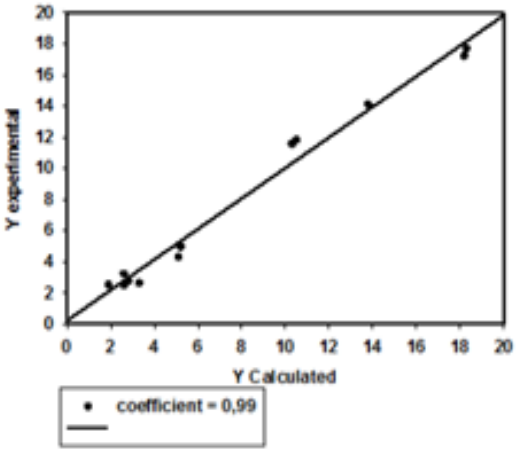

Fig. 7. Experimental vs. Predicted permeabilities

The optimal zones correspond to the red zones on the coloured isoreponse lines show in Fig. 9. We can clearely see the evolution of the response (permeability).

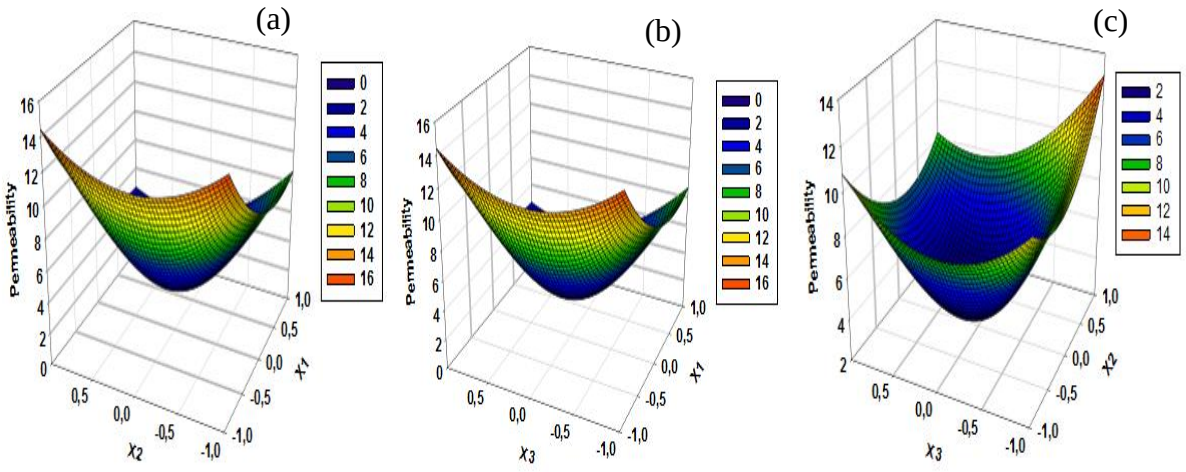

Fig. 8 (a, b, c). Reponse surfaces (X_1: Solvent, X_2: Nano-ZnO, X_3: Casting speed)

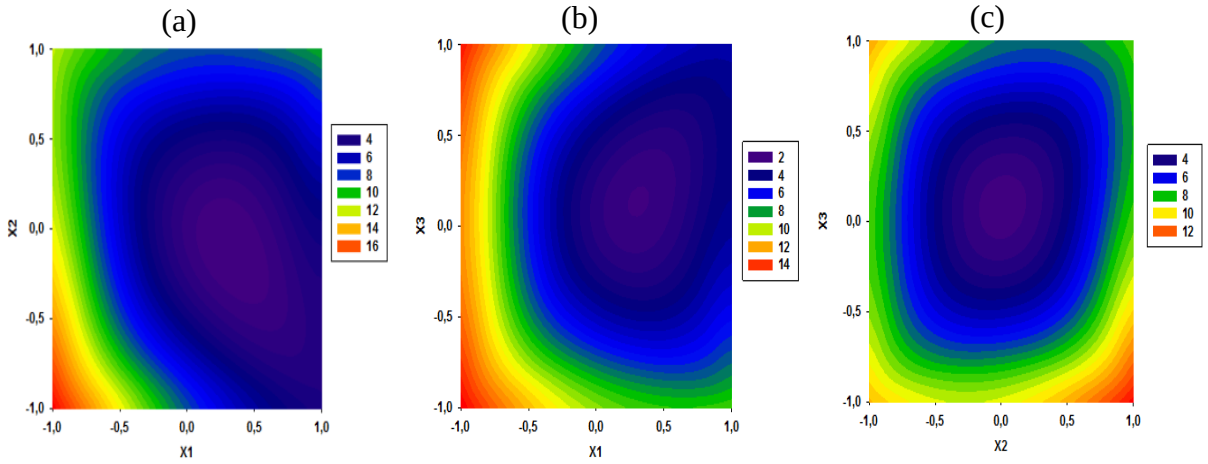

Fig. 9. Coloured contour plot : (**a**) Solvent and ZnO, (**b**) Solvent and Casting speed, (**c**) Solvent and Casting speed

For both solvent dose and ZnO NPs, solvent dose and casting speed, ZnO NPs and casting speed, a local maxima of permeability of 16 $L.h^{-1}.m^{-2}.bar^{-1}$, 14 $L.h^{-1}.m^{-2}.bar^{-1}$, 12 $L.h^{-1}.m^{-2}.bar^{-1}$ are found at the coded point X_1X_2 (-1, -1) ; X_1X_3 (-1, -1) & (-1, +1) ; X_2X_3 (+1, -1).

These results show that, the permeability decreases with increasing ZnO NPs. This is due to an increase in the viscosity of the collodion which slows the growth of the porous structures, generating the obtaining of smaller pores than with a lower concentration (0.5% by mass) [8, 22]. Because of the fact that the coefficient of the $X_1X_2X_3$ of the model equation cannot be neglected, the best response range can be obtained by analyzing the response surface plots. A maximum permeability (17.7 $L.h^{-1}.m^{-2}.bar^{-1}$) was observed at fixed solvent (70%), ZnO NPs (0.5%) and casting speed (20mm/s).

4 Conclusion

A serie of membranes was prepared by a phase-inversion method. The preparation and characterization of PES membrane have been investigated in the presence of PVP as porogen. The PVP and ZnO NPs strongly affect the membrane properties. The porosity of

membrane is improved by adding PVP and ZnO NPs. Synthesis process parameters namely solvent, nanoparticles and casting speed were considered to optimize the permeability. The multiple correlation coefficient of determination R2 was 99.97%, showing that the actual data fitted well with the predicted data. We have shown that it is possible to include nanoparticles in matrix of polyethersulfone membrane to modify its properties, giving membranes more permeable to water than a pure PES membrane without compromising the rejection performance significantly.

Acknowledgement
Dr Patrick Loulergue is gratefully acknowledged for technical assistance in membrane development.

References :

[1] Xu Z. L., Qusay F. A., Effect of polyethylene glycol molecular weights and concentrations on polyethersulfone hollow fiber ultrafiltration membranes, *Journal Applied Polymer Science*, Vol. 91, No. 5, 2004, pp. 3398-3407.

[2] Li Y., Cao C., Chung T. S., Pramoda K. P., Fabrication of dual-layer polyethersulfone (PES) hollow fiber membranes with an ultrathin dense-selective layer for gas separation, *Journal Membrane Science*, Vol. 245, No. 1, 2004, pp 53 – 60

[3] Boussu K., Vandecasteele C., Van der Bruggen B., Study of the characteristics and the performance of self-made nanoporous polyethersulfone membranes, *Polymer*, Vol. 47, No. 10, 2006, pp 3464-3476.

[4] Jing-Feng L., Zhen-Liang X., Hu Y., Li-Yun Y., Min L., Effet of TiO_2 nanoparticles on the surface morphology and performance of microporous PES membrane, *Applied Surface Science*, Vol. 255, No. 9, 2009, pp. 4725-4732

[5] Van de Witte P., Dijkstra P. J., Van den Berg J. W. A., Feijen J. S., Phase separation processes in polymer solutions in relation to membrane formation, *Journal of membrane science*, Vol. 117, 1996, pp. 1-31

[6] Barth C., Goncalves M. C., Pires A. T. N., Roeder J., Wolf B. A., Asymmetric polysulfone and polyethersulfone membranes: effects of thermodynamic conditions during formation on their performance, *Journal of Membrane Science*, Vol. 169, No. 2, 2000, pp. 287-299

[7] Peyravi M., Rahimpour A., Jahanshahi M., Javadi A., Shockravi A., Tailoring the surface properties of PES ultrafiltration membranes to reduce the fouling resistance using synthesized hydrophilic copolymer, *Microporous and Mesoporous Materials*, Vol. 160, 2012, pp. 114-125.

[8] Rajabi H., Ghaemi N., Madaeni S. S., Daraei P., Astinchap B., Zinadini S., Razavizadeh S. H., Nano-ZnO embedded mixed matrix polyethersulfone (PES) membrane : Influence of nanofiller shape on characterization and fouling resistance, *Applied Surface Science*, Vol. 349, 2015, pp. 66-77.

[9] Ahmed F., Santos C., Mangadlao J., Advincula R. and Rodrigues D. Antimicrobial PVK:SWNT nanocomposite coated membrane for water purification: Performance and toxicity testing, *Water Research*, Vol. 47, No. 12, 2013, pp. 3966–3975

[10] Zhao C., Xue J., Ran F., Sun S., Modification of polyethersulfone membranes—A review of methods, *Progress in Materials Science*, Vol. 58, No. 1, 2013, pp. 76–150

[11] Arkhangelsky E., Kuzmenko D., Norm V. Gitis, Vinogradov M., Kuiry S., Gitis V., Hypochlorite cleaning causes degradation of polymer membranes, *Tribol Lett*, Vol. 28, 2007, pp. 109–116

[12] Yadav K., Morison K., Staiger M. P., Effects of hypochlorite treatment on the surface morphology and mechanical properties of polyethersulfone ultrafiltration membranes, *Polymer Degradation and Stability*, Vol. 94, No. 11, pp. 1955-1961

[13] Rahimpour A. and Madaeni S. S., Polyethersulfone (PES)/cellulose acetate phthalate (CAP) blend ultrafiltration membranes: Preparation, morphology, performance and antifouling properties, Journal of Membrane Science, Vol. 305, No. 1-2, 2007, pp. 299-312

[14] Rahimpour A., UV photo-grafting of hydrophilic monomers onto the surface of nano-porous PES membranes for improving surface properties, Desalination, Vol. 265, No. 1-3, 2011, pp : 93–101

[15] Abu S. M. N., Khayet M., Hilal N., Comparaison of two different UV-grafted nanofiltration membranes prepared for reduction of humic acid fouling using acrylic acid and N-vinylpyrrolidone, Desalination, Vol. 287, 2012, pp. 19-29

[16] Shi Q., Su Y., Chen W., Peng J., Nie L., Zhang L., Jiang Z., Grafting short-chain amino acids onto membrane surfaces to resist protein fouling. *Journal of Membrane Science*, Vol. 366, 2011, pp. 398-404

[17] Kim J. and Van Der Bruggen B., The use of nanoparticles in polymeric and ceramic membrane structures : review of manufacturing procedures and performance improvement for water treatment, *Environmental Pollution*, Vol. 58, No. 158, 2010, pp. 2335-2349

[18] Liang S., Xiao K., Mo Y., Huang X., A novel ZnO Nanoparticle blended polyvinylidene fluoride membrane for anti-irreversible fouling, *Journal of Membrane Science*, Vol. 394, 2012, pp. 184-192

[19] Hong J., He Y., Effects of nano sized zinc oxide on the performance of PVDF microfiltration membranes, *Desalination*, Vol. 302, 2012, pp. 71-79

[20] Shen L., Bian X., Lu X., Shi L., Liu Z., Chen L., Hou Z., Fan K., Preparation and characterization of ZnO/polyethersulfone (PES) hybrid membranes, *Desalination*, Vol. 293, 2012, pp. 21-29

[21] Suhana Jalil., Development of Polyethersulfone Nanofiltration Hollow Fiber Membrane for Cyclodextrin Enzyme Separations, Department of Bioprocess Engineering, Universiti Teknologi Malaysia, *Msc. Thesis*, 2004

[22] Balta S., Sotto A., Luis P., Benea L., Van der Bruggen B., Kim J., A new outlook on membrane enhancement with nanoparticles: The alternative of ZnO, *Journal of Membrane Science*, Vol. 389, 2012, pp. 155-161.

[23] Li J-F., Zhen-Liang X., Hu Y., Li-Yun Y., Min L., Effet of TiO_2 nanoparticles on the surface morphology and performance of microporous PES membrane. *Applied Surface Science*, Vol.255, No. 9, 2009, pp. 4725-4732.

[24] Mohammad A. W., Teowa Y. H., Anga W. L., Chunga Y. T., Oatley-Radcliffec D. L., Hilalcd N., Nanofiltration membranes review: Recent advances and future prospects. *Desalination*, Vol.356, 2015, pp. 226-254.

[25] Wanyi F., Christina C., Xiaosong W., Wen Z., Visualizing and Quantifying Nanoscale Hydrophobicity and Chemical Distribution of Modified Polyethersulfone (PES) Membranes. *Nanoscale*, Vol. 9, No. 40, 2017, pp. 15550-15557

[26] Ndjeumi C. C., Măicăneanu A, Bike Mbah J. B., Mouthe A. G., Kamga R., Assessment of Physico-Chemical Parameters for Humic Acids Adsorption on Alumina, *Chemistry Journal*, Vol. 1, No. 4, 2015, pp. 133-138

[27] Goupy J., *Plans d'expériences : les mélanges*, Dunod, Paris, 2000, pp. 285,

[28] Dagnelie P., *Principes d'expérimentation : Planification des expériences et analyse de leurs résultats*, Presses agronomiques, Gembloux, 2012, pp. 413

[29] Khan M., Tahir M. N., Adil S. F., Khan H. U., Siddiqui M. R. H., Al-warthan A. A., Tremel W., Graphene based metal and metal oxide nanocomposites: synthesis, properties and their applications. *Journal Materials Chemistry A*., Vol. 3, 2015, pp. 18753-18808

[30] Gzara L., Zulfiqar A., Rehan, Sher B., Khalid A. A., Mohammad H. A., El-Shahawi M. S., Muhammad I. R., Alberto F. ; Enrico D., Abdullah M. A., Preparation and characterization of PES-cobalt nanocomposite membranes with enhanced anti-fouling properties and performances. *Journal of the Taiwan Institute of Chemical Engineers*, Vol. 65, 2016, pp. 405-419

[31] Zhen-Liang Xu and F. Alsalhy Qusay, Polyethersulfone (PES) hollow fiber ultrafiltration membranes prepared by PES/non-solvent/NMP solution, *Journal of Membrane Science*, Vol. 233, No. 1-2, 2004, pp. 101-111

[32] Haaland P. D., *Statistical Problem Solving, Experimental Design in Biotechnology*, Marcel Dekker, New York, 1989, pp. 1-18,

[33] Muller M., *Basic principles of membrane technology*. Kluwer Academic Publishers, 1996, pp. 564

[34] Bouyer D., Faur C., Pochat C., *Procédés d'élaboration de membrane par préparation de phases*, Techniques de l'ingénieur, Article / Réf : J2799 V1, 2011, pp. 36.